ROYAL SOCIETY
OF CHEMISTRY

EDGE ARTICLE

Check for updates

A preliminary profile of RNA bound on the cell surface

Xiangru Zhang,†[ab] Weiwei Li,†[cd] Guomiao Liao,[d] Yu Zhang,[ad] Jing Sheng,[ab] Zhenhao Long,[ab] Nan Zhang,[ab] Ji Zhu,[c] Xiangjun Liu [ID] [ab] and Dihua Shangguan [ID] *[abd]

Molecules on the cell surface play crucial roles in cellular material exchange, molecular recognition, signal transduction, migration, growth, differentiation, and pathological processes. Due to the lack of simple and effective methods, little is known about the nucleic acids on the cell surface. In this paper, using synthetic DNA G4 as probes, we found that a significant amount of RNA was associated with the cell surface during cell culture. Both RNA and DNA G4 were found to bind RNA-binding proteins on the cell surface, such as nucleolin. The amount of RNA bound to the cell surface varies greatly among different cell lines, and increases over time after treatment with proteases or RNase A. The RNA bound on the cell surface is primarily internal cellular RNA fragments between 20–100 nt in length, including microRNAs. Addition of RNase A in the culture medium to remove cell surface RNA can inhibit cell growth and promote cell migration. These results provide a preliminary understanding of RNA bound to the cell surface and offer new perspectives on the metabolism and function of nucleic acids inside and outside the cells.

Introduction

The cell surface is a crucial interface between the interior and exterior of the cells. As is well known, the outer surface of cells has many bioactive molecules, including proteins, glycans, lipids, and their chemically modified variations. These bioactive molecules are essential for the cell surface functions, *e.g.*, extracellular signal sensing, extracellular matrix anchoring, and antigen presentation. However, as an important biomacromolecule for cells, the distribution and function of nucleic acids on the cell surface are still poorly understood. Reports on membrane-bound nucleic acids on live cells date back as early as 2004. E. S. Morozkin reported that DNA and RNA released by cultured eukaryotic cells could bind to the cell surface.[1] In 2011, the first membrane-bound RNAs identified on bacteria were non-coding, transcribed in the same operon as the genes for transmembrane proteins. After transcription, the

RNA and proteins form a ribonucleoprotein complex that integrates into the cell membrane.[2] In 2012, it was demonstrated that *t*RNA can bind to membrane lipids of HeLa cells under physiological ionic conditions.[3] In 2013, we reported the general binding of intramolecular G-quadruplex (G4) DNA on live cells.[4] In 2020, using RNA sequencing and RNA-FISH, Huang *et al.* identified membrane-associated extracellular RNAs (maxRNAs and nuclear-encoded RNA) on human circulating blood cells, mostly on monocytes. They observed considerable variation in maxRNAs among different cell types and within the same type, suggesting a potential role for maxRNAs in cell–cell communication.[5] In 2021, Flynn, R. A. first reported that small RNAs in cancer and embryonic stem cells can be *N*-glycosylated, forming glycoRNAs that were localized on the cell surface.[6] This discovery quickly attracted great attention. Soon, the cell surface glycoRNAs were identified as critical for neutrophil recruitment to inflammatory sites by Zhang N. *et al.* and glycoRNA expression required the mammalian homologs of the sid-1 RNA transporter. Neutrophil glycoRNAs are predominantly on the cell surface, important for neutrophil–endothelial interactions, and can be recognized by P-selectin.[7] Based on the important functions of glycoRNAs, two sensitive *in situ* visualization strategies for glycoRNAs on living cell membranes were recently evaluated. The number of glycosylation sites on a single RNA, the spatial distributions of glycoRNAs on the cell surface and their colocalization with lipid rafts, and the intracellular trafficking of glycoRNAs through SNARE protein-mediated secretory exocytosis were revealed by these strategies.[8,9] These studies suggest that cell surface glycoRNA is inversely

[a]*Beijing National Laboratory for Molecular Sciences, Key Laboratory of Analytical Chemistry for Living Biosystems, CAS Research/Education Center for Excellence in Molecular Sciences, Institute of Chemistry, Chinese Academy of Sciences, Beijing, 100190, China*

[b]*School of Chemical Sciences, University of Chinese Academy of Sciences, Beijing, 100049, China*

[c]*Zhejiang Key Laboratory of Radiation Oncology, Zhejiang Cancer Research Institute, Zhejiang Cancer Hospital, Hangzhou Institute of Medicine (HIM), Chinese Academy of Sciences, Hangzhou, Zhejiang 310022, China*

[d]*School of Molecular Medicine, Hangzhou Institute for Advanced Study, University of Chinese Academy of Sciences, Hangzhou, 310013, China*

† X. Z. and W. L. contributed equally to this work.

associated with tumor malignancy and metastasis and may mediate cell–cell interactions during the immune response.[9]

At present, the primary methods for studying cell surface nucleic acids focus on sequencing[5,10] and hybridization based nucleic acid probes.[8,9] These methods can detect specific nucleic acid sequences but cannot conveniently and quickly reflect the universal binding of nucleic acids on different cell surfaces. Due to the lack of effective and universal detection methods, the understanding of cell surface nucleic acids is still very limited. Therefore, qualitative and quantitative studies of RNA on the cell surface are important and valuable for the study of the physiological functions of RNA on the cell surface.

Here, we present a relatively simple approach for investigating RNAs bound on the cell surface, utilizing dye-labeled DNA G4 sequences as probes. With this method, we studied the RNAs bound on various cell lines. Employing a G4 DNA probe, VEGF G4, we explored the dynamics of RNAs bound on the cell surface and preliminarily revealed the potential protein targets of RNAs on the cell surface. We extracted the RNAs from the cell surface, analyzed their length distribution by agarose gel electrophoresis and CE, and then sequenced them *via* the DNBSEQ platform (BGI Group, Shenzhen, China). Furthermore, we confirmed the binding of three RNAs identified in sequencing data to the cell surface. We further investigated whether cell functions such as proliferation and migration were affected by the removal of RNA bound on the cell surface.

Results and discussion

Binding of FAM-labeled oligo-DNA on the cell surface

Nucleic acids are polyanions that can non-specifically bind to positively charged molecules or regions on the surface of live cells. After incubating the fluorescently labeled nucleic acid sequences with living cells, a certain amount of fluorescent sequences will bind to the cell surface depending on the condition of the cell surface. Therefore, in the specific binding experiments of nucleic acid sequences, such as aptamers, against live cells, excess herring sperm DNA (HS-DNA, 0.1 mg mL^{-1}) or t-RNA is usually added to inhibit this non-specific binding.[11] HS-DNA, consists of a large number of random-sequence DNA fragments that can bind to the positively charged regions on the cell surface through electrostatic interactions, thereby competitively inhibiting the non-specific adsorption of functional nucleic acids. G4s are four-stranded structures adopted by guanine-rich nucleic acids, which are widely considered to play important roles in the regulation of genomic function, such as telomere maintenance, transcription and translation.[12] Different G4s have been reported to bind a wide range of proteins within cells.[13,14] Our previous work has demonstrated that DNA G4 sequences with a parallel structure have the general binding activity to certain surface proteins of live cells. Different sequences have different binding affinities, and different cells can bind different amounts of G4 sequences.[4] To further understand the specific and non-specific binding of synthetic oligo-DNA to cells, we conducted flow cytometry assay on cells after incubation with FAM-labeled DNA G4 sequences, VEGF G4 and AS1411, as well as a FAM-labeled non-G4 DNA

sequence, VEGF-4T (four G nucleotides of VEGF G4 was replaced with four T) (Table S1). For VEGF-4T, incubation without HS-DNA resulted in minimal binding to LoVo and PC-3 cells, with fluorescence intensities barely above background levels, and this was slightly reduced with HS-DNA present. Conversely, VEGF-4T exhibited substantial binding to MCF-7R cells, leading to intense fluorescence, which was markedly diminished to just above background levels in the presence of HS-DNA. Staining experiments using the anionic dye ANS (1-anilinonaphthalene-8-sulfonate) demonstrated that the surface of MCF-7R cells had a higher positive charge density compared to other cells (Fig. S1), which accounts for the aforementioned observations. For the G4 sequences VEGF G4 and AS1411, extensive binding to all tested cell lines was noted following incubation without HS-DNA, but this binding was considerably diminished by the presence of HS-DNA, remaining, however, significantly stronger than that observed with the non-G4 sequence (Fig. 1A). The HS-DNA concentration gradient experiments revealed that 0.1 mg mL^{-1} HS-DNA is sufficient to fully inhibit the non-specific binding of G4s to cells (Fig. S2). These results suggest that the synthetic non-G4 sequence exhibits strong non-specific binding to MCF-7R cells, which can be competitively inhibited by HS-DNA, whereas its non-specific binding to other cell types is weaker. In contrast, G4 DNA sequences demonstrate strong binding to all tested cells, which can be partially reduced by HS-DNA, confirming the specific binding of G4 on the cell surface. In order to minimize non-specific adsorption of DNA and RNA to cells, all subsequent binding experiments were carried out in the presence of 0.1 mg mL^{-1} HS-DNA.

FAM-labeled G4 sequences as probes for indicating cell surface RNA

The above G4 binding experiments neglected the influence of pre-bound DNA and RNA on the cell surface during cell culture on the subsequent binding of synthesized G4 sequences. Thus, the FAM-labeled G4 binding experiments were further performed with LoVo cells treated with DNase I, RNase H and RNase A, respectively. The fluorescence from all tested G4 sequences on RNase A-treated cells was notably higher than that on untreated ones (Fig. 1B), suggesting abundant RNA pre-bound on the cell surface that may have occupied the DNA G4 binding sites. No significant binding changes were observed on cells with DNase I or RNase H treatments, suggesting a few RNA–DNA hybrids or DNA sequences pre-bound on the surface. In addition, the strong binding of a LoVo cell-specific aptamer (yly12, a non-G4 DNA sequence targeting L1CAM[11]) and the weak binding of a control sequence (VEGF-4T) to LoVo cells remained consistent regardless of the treatment with DNase I, RNase H, or RNase A, suggesting the unique interaction of FAM-labeled DNA G4 sequences with the surface of cells treated with RNase A.

Similar results were also observed on HUVEC cells after treatment with RNase H and RNase A (Fig. S3). PI (propidium iodide) staining experiments ruled out the possibility that RNase A treatment increases cell permeability (Fig. S4). To
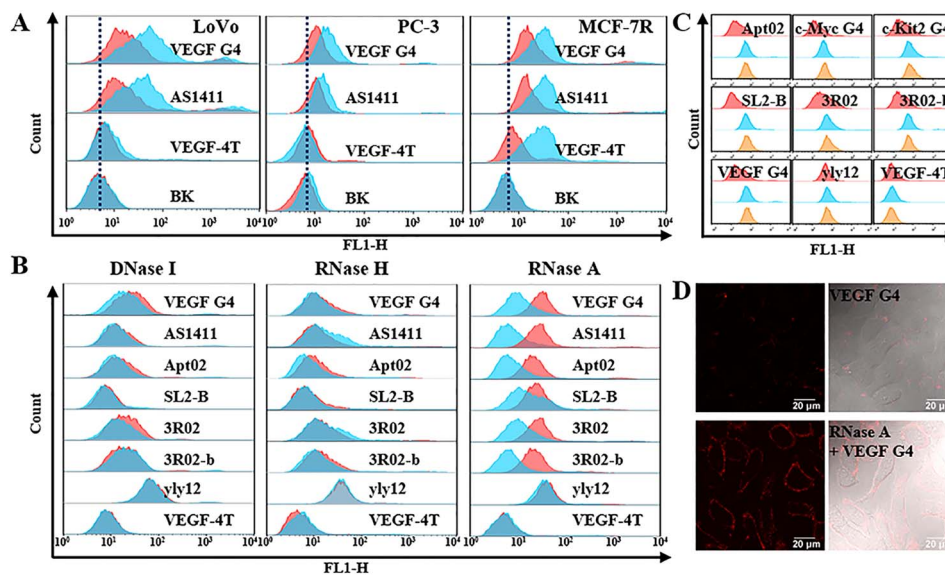
Fig. 1 (A) Flow cytometry analysis of FAM-labeled G4 sequence (VEGF G4, AS1411, 200 nM) and non-G4 sequence (VEGF-4T) binding on LoVo, PC-3, and MCF-7R cells in the presence or absence of HS-DNA (cyan blue, no HS-DNA; red, 0.1 mg mL^{-1} HS-DNA, BK, cells only (background fluorescence)). (B) Flow cytometry assay of different FAM-labeled DNA sequence (VEGF G4, AS1411, Apt02, SL2-B, 3R02, 3R02-b, 200 nM) binding on LoVo cells with and without treatment with DNase I, RNase H or RNase A (aptamer yly12 and VEGF-4T, control sequences; red, cells treated with DNase I, RNase H or RNase A; cyan blue, untreated cells). (C) Flow cytometry assay of different FAM-labeled DNA sequence (Apt02, c-Myc G4, c-Kit2 G4, SL2-B, 3R02, 3R02-b, VEGF G4) (200 nM) binding on RNase A-treated cells, with specific attention to samples washed either once or five times (aptamer yly12 and VEGF-4T, control sequences; red, untreated cells; blue and orange, RNase A-treated cells with once or five washes after DNA binding). (D) Confocal microscopy images of FAM-VEGF G4 (400 nM) binding to LoVo cells, with or without RNase A treatment.

exclude the possibility that residual RNase A on cells might enhance the binding of G4 sequences to cells, and to verify if increased G4 binding to RNase A-treated cells is specific, fluorescence intensities of FAM-labeled DNA sequences (VEGF G4, Apt02, 3R02, 3R02-b, SL2-B, c-Kit2 G4, c-Myc G4 and yly12) on RNase A-treated LoVo cells were compared following 1 or 5 washes with pre-cooled washing buffer at 4 °C (Fig. 1C). The results showed that G4 fluorescence intensities remained consistent between 5 and 1 washes. The confocal imaging revealed stronger fluorescence on RNase A-treated LoVo cells stained with FAM-labeled VEGF G4 compared to untreated cells (Fig. 1D). Additionally, competition binding assays showed that *t*RNA exhibited significant competition with the binding of FAM-labeled VEGF G4 to RNase A-treated LoVo cells, whereas it only caused slight competition for the binding of FAM-labeled VEGF G4 to untreated LoVo cells (Fig. S5). These results indicate that the G4 probe and cell surface RNA bind to the same site on the cell surface.

GelRed is an ultra-sensitive, extremely stable and environmentally safe fluorescent nucleic acid dye for staining dsDNA, ssDNA or RNA in agarose gels or polyacrylamide gels. Because its penetration into live cells is difficult, it was used to stain nucleic acids on the cell surface. The flow cytometry assay revealed a marked reduction in GelRed fluorescence intensity on LoVo cells treated with RNase A compared to untreated cells, whereas no significant difference in fluorescence was observed between DNase I-treated and untreated cell surfaces (Fig. S6A). Confocal imaging also showed a decrease in GelRed

fluorescence on the surface of LoVo cells upon the RNase A treatment (Fig. S6B). These results further corroborated the aforementioned conclusion that a substantial amount of RNA is associated with the cell surface during cell culture, whereas DNA is minimally present. Although GelRed can reflect the changes in the amount of RNA on the cell surface after treatment with RNase A, its fluorescence intensity on cells and the intensity change after treatment with RNase A were much weaker than that of the FAM-labeled synthesized G4 sequences. This set of results suggests that dye-labeled G4 sequences can serve as probes for indicating cell surface RNA.

Cell surface bound RNA on different cell lines

Using FAM-labeled G4 sequences as probes (VEGF G4, c-Kit2 G4, c-Myc G4, AS1411, Apt02, 3R02, 3R02-b, and SL2-B), we investigated the RNA bound on the surface of various types of cells (Fig. 2A). Following incubation with various probes, we observed varying levels of fluorescence enhancement in all RNase A-treated cells compared to their untreated controls. Notably, HeLa, HUVEC, PC-3, and MCF-7R cells demonstrated significant fluorescence enhancement, whereas K562 and Jurkat E6-1 cells exhibited only a slight increase in fluorescence. These findings suggest that the amount of RNA bound on the cell surface varies among different cell types. Moreover, the results indicate that different G4 probes exhibit varying binding ability to the RNase A-treated cell surface. To identify a G4 probe with a strong affinity for the cell surface, we investigated the binding curves (Fig. 2B) of several G4 probes on RNase A-treated
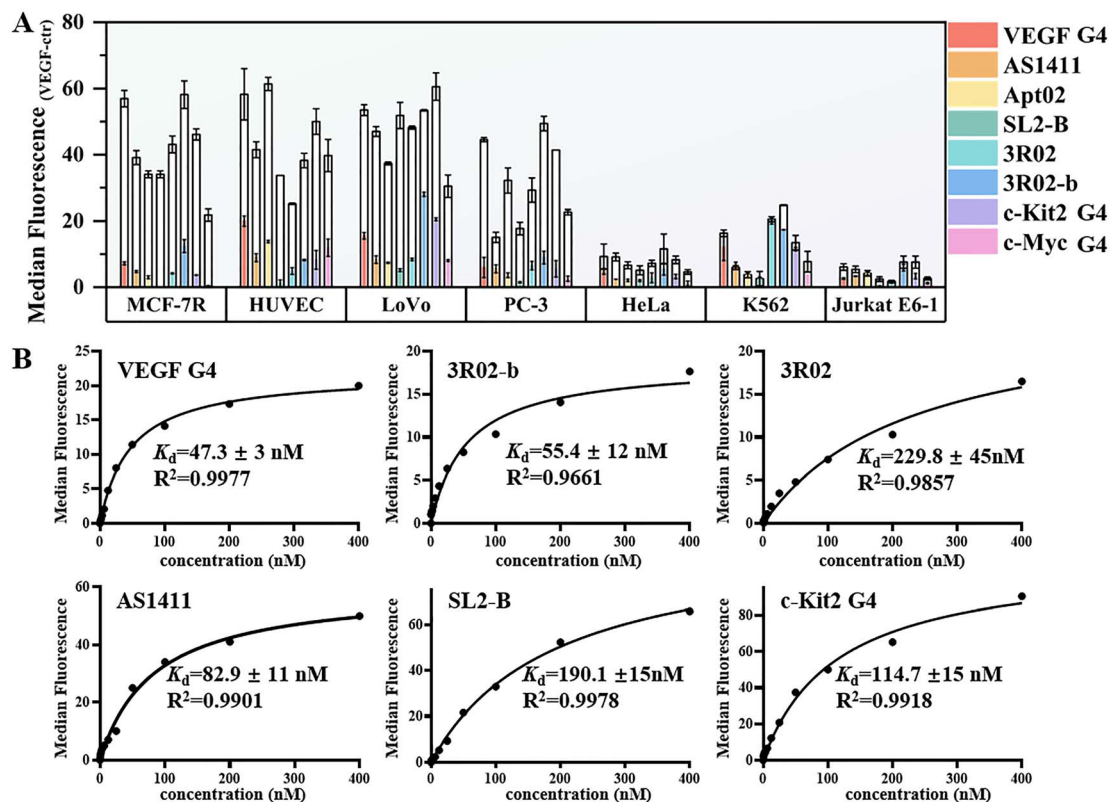
Fig. 2 (A) The binding of various FAM-labeled G4 sequences (200 nM) on different cell lines with and without treatment with RNase A. ($n = 3$; bars: SEM). The ordinate represents the difference in median fluorescence intensity between cells incubated with G4 and those incubated with a control sequence. Filled colors denote cells untreated with RNase A, and unfilled colors denote cells treated with RNase A. (B) Binding curves of FAM-labeled G4 sequences, VEGF G4, 3R02, 3R02-b, AS1411, SL2-B and c-Kit2 G4 on RNase A-treated LoVo cells at 4 °C.

LoVo cells, which had previously demonstrated notable fluorescence enhancement. Among these G4 sequences, VEGF G4 demonstrated the strongest binding affinity, with the lowest apparent equilibrium dissociation constant (K_d) of 47.3 nM. Subsequent efforts to enhance probe affinity through mutation experiments focused on the VEGF G4 sequence; however, none of the modified probes achieved higher affinity than the original VEGF G4 probe (for more details, please refer to the SI). Therefore, subsequent research primarily uses VEGF G4 as the probe.

### The binding targets of cell surface bound RNA and G4 probes

Our previous study has demonstrated that the binding targets of DNA G4 sequences on the cell surface are certain cellular surface proteins, for example, nucleolin.[4] The above results have suggested that cell surface adsorbed RNA may bind to the same protein sites as the DNA G4 sequences. To test this, we detached LoVo cells with trypsin and proteinase K respectively to remove the cell surface proteins, and then treated cells with RNase A and incubated them with FAM-labeled G4 sequences; the EDTA detached cells were used as a positive control. Flow cytometry analysis revealed that the positive control cells exhibited strong fluorescence, while cells treated with 0.05% trypsin or proteinase K showed minimal fluorescence, akin to the background levels of the ctr sequence (Fig. 3A). This result

confirmed that the binding targets of cell surface bound RNA and G4 probes are membrane proteins.

Putative G4-forming sequences are highly prevalent in the genome and transcriptome of various organisms from viruses, prokaryotes to eukaryotes.[12,15] Emerging research shows that G4s are involved in various biological processes, such as transcription, replication, translation, recombination, and telomere maintenance.[16] These processes involve the interaction of various proteins with G4s.[17] In addition, G4 structures are usually found in aptamers, and synthetic oligonucleotides specifically bound a variety of protein targets selected by the SELEX technique.[18] RNA is a vital part of processes such as transcription, translation, and cellular functions, and thus a large class of over 2000 proteins have been found to interact with RNA in all manner of RNA-driven processes.[19,20] Some RNA-binding proteins (RBPs) have been reported to bind DNA G4, such as Arg-Gly-Gly (RGG)-containing proteins, the second most common class of RNA-binding proteins in the human genome.[21] This family of proteins contains relatively closely spaced RGG and/or RG repeats, and the length of spacing and the identity of amino acids between the adjacent RGG and/or RG repeats vary. The RGG motifs are reported to bind RNA, as well as DNA- and RNA- G4 structures.[21–26] Although most RBPs and G4-binding proteins are present in cells, some are also found on the cell surface—nucleolin, for instance,[4,19,23] a recent
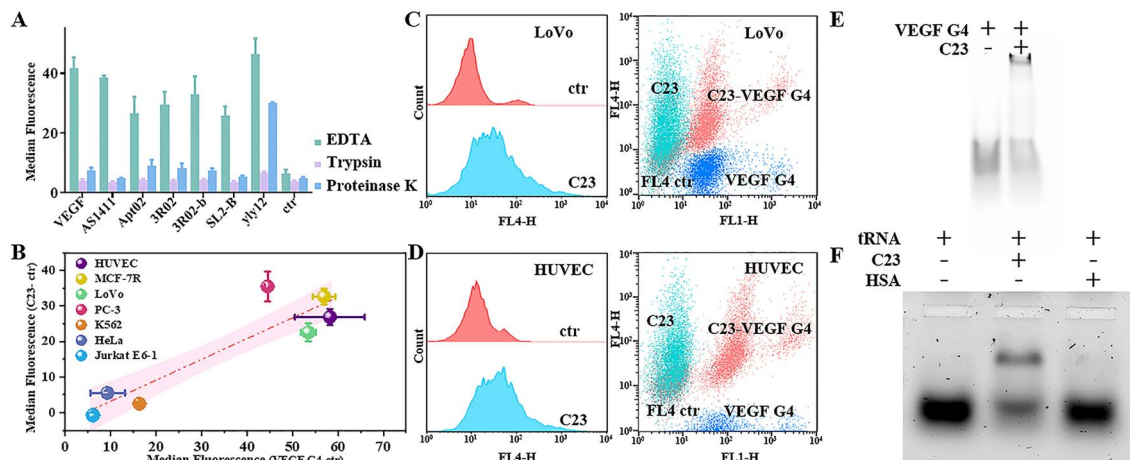
Fig. 3 (A) Flow cytometry assay of G4 sequence (VEGF G4, AS1411, Apt02, 3R02, 3R02-b, and SL2-B) (200 nM) binding on RNase A-treated LoVo cells after detachment by using EDTA (pale green), 0.05% trypsin (azure) and proteinase K (light purple) at 37 °C (ctr: yly12, VEGF-4T; $n = 3$; bars: SEM). (B) Correlation between nucleolin (C23) expression on different cells (HUVEC, MCF-7R, LoVo, PC-3, K562, HeLa and Jurkat E6-1) and the increase in fluorescence values for VEGF G4 (200 nM) binding. (C and D) Flow cytometry assay of LoVo cells (C) and HUVEC cells (D) stained by anti-C23 antibodies (Cy5, FL4-H, left), and co-stained by anti-C23 antibody (FL4-H) and VEGF G4 (FAM, FL1-H, right), gray: single-stained with normal mouse IgG1; blue: single-stained with VEGF G4; azure: antibody single-stained with anti-C23; pink: costained with VEGF G4 and anti-C23 antibody. (E) EMSA analysis (polyacrylamide gel) of the binding between nucleolin (C23 1000 nM) and VEGF G4 (200 nM). (F) EMSA analysis (agarose gel) of the binding between tRNA (10 μg mL^{-1}) and nucleolin (200 μg mL^{-1}) or control protein HSA (200 μg mL^{-1}).

study revealed that a large number of RBPs also exist on the cell surface.[27] Therefore, RNA binds to cell surface RBPs, which potentially also interact with G4s. When RNA is removed from the cell surface by RNase A, the vacated RGG-like G4 binding sites become accessible, resulting in the increased G4 binding observed in the aforementioned experiments.

To prove this hypothesis, cell surface proteins that bind G4s were pulled down using VEGF G4 and identified via a SILAC (Stable Isotope Labeling by Amino acids in Cell culture)-based quantitative proteomic assay.[28] In this experiment, we chose a DNA aptamer, BG2, as the control sequence, which exhibits specific binding to LoVo cells but does not compete with VEGF G4 for cell binding[18] (Fig. S7A). Furthermore, cells treated with RNase A could not increase the cell binding of BG2 (Fig. S7B). Briefly, biotin-labeled VEGF G4 and BG2 were incubated and bound with LoVo cells cultured with lysine and arginine labeled by using light and heavy isotopes respectively (Fig. S7C). After in situ formaldehyde cross-linking, DNA-protein complexes were pulled-down from the cell lysate with streptavidin beads. The complexes were simply isolated by SDS-PAGE, digested in a gel and analyzed by LC-MS/MS. In the candidate proteins (Table S4), four RNA-binding proteins, sarcoma fusion/liposarcoma transfer protein (FUS/TLS),[29] Ewing's tumor protein (EWS), nucleolin (C23), and nucleolar phosphoprotein (B23) were found to have protein abundance ratios (Heavy-G4/Light-Ctr) greater than 1.3. The EWS oncogene contains an N-terminal transcription activation domain and a C-terminal RNA-binding domain. The RGG domain of the C-terminal in EWS was reported to bind to DNA and RNA G4 structures.[26,30] Nucleolin is a well-known G4 binding protein highly expressed on many tumor cell surfaces;[19] both its RGG domain and RNA recognition motif are reported to be responsible for G4 binding and

folding.[23] It has also been identified as a direct binding partner of 5′-tRFCys (a cysteine tRNA fragment).[31] TLS/FUS is a multifunctional DNA/RNA-binding protein expressed in the cytoplasm and could specifically bind to G4 through the RGG motif.[29,32] Nucleolar phosphoprotein B23/nucleophosmin (NPM1) is a nucleocytoplasmic shuttling protein that plays a key role in several cellular functions. It is ubiquitously expressed in tissues and can be found in the nucleolus, nucleoplasm, cytoplasm, and extracellular environment and can bind parallel G4, DNA and RNA.[33–35]

It is worth noting that the four proteins were identified with a moderate-to-low heavy/light ratio, and only one peptide was found for (FUS/TLS) and EWS. This could be attributed to (1) the low affinity between the VEGF G4 sequence and cell surface proteins ($K_d \geq 47$ nM) leading to a small amount of pulled-down proteins; (2) the large variety (thousands of types) yet low abundance of cell surface RBPs resulting in a low amount of pulled-down proteins;[27] (3) and the non-specific binding of numerous intracellular nucleic acid-binding proteins to the VEGF G4 and BG2 sequences causing a reduced ratio. To further ascertain the relationship of the identified proteins with RNA bound on the cell surface, the expression of nucleolin (C23), B23, and TLS/FUS on the surface of different cell lines (LoVo, HUVEC, PC-3, MCF-7R, HeLa, K562 and Jurkat E6-1) was analyzed by flow cytometry using their specific monoclonal antibodies. Since antibodies for detecting EWS on the cell surface were not available, the expression level of EWS could not be determined. Nucleolin (C23) was found to be highly expressed on the surface of HUVEC, MCF-7R and PC-3 cells, moderately expressed on LoVo, HeLa and K562 cells, and not expressed on Jurkat E6-1 cells (Fig. 3C, D and S8). The expression level of nucleolin on the surface of these cells showed

a positive correlation with the binding of VEGF G4 to these cells after RNase A treatment (Fig. 3B). The dual-staining experiment with anti-C23 antibody and FAM-labeled VEGF G4 also demonstrated the correlation between nucleolin expression and VEGF G4 binding on HUVEC and LoVo cells (Fig. 3C and D). Nucleolar phosphoprotein (B23) was found to be slightly expressed on the surface of MCF-7R, PC-3, LoVo, HUVEC and HeLa cells, while FUS/TLS was also slightly expressed on LoVo, HUVEC and MCF-7R cells (Fig S8 and S9). The expression of both proteins is also correlated to some extent with the binding of VEGF G4 on these cells. The direct interactions between nucleolin (C23) and both FAM-labeled VEGF G4 and tRNA were also demonstrated via Electrophoretic Mobility Shift Assay (EMSA) (Fig. 3E and F). These results suggest that these RBPs expressed on the cell surface could be potential targets of DNA G4s. Due to the not-so-strong binding affinity of VEGF G4 to cells and the vast yet low-abundance repertoire of RBPs on the cell surface, it is possible that numerous RBPs expressed on the cell surface remain unidentified in this experiment. Furthermore, the types and quantities of RBPs expressed on the cell surface may differ among various cell types. The results we have obtained so far explain why the amount of DNA G4 bound to cells treated with RNase A increases, and preliminarily demonstrate the feasibility of using DNA G4 as a probe to study the adsorption of RNA by proteins on the cell surface.

The change in RNA bound on cell surfaces under different culture conditions

To gain insights into the dynamics of RNA bound to the cell surface during culture, we detached LoVo cells using 0.05% trypsin and then cultured them in an RPMI-1640 medium supplemented with 10% fetal bovine serum (FBS) for various periods. Following this, we measured the binding of VEGF G4 to LoVo cells with and without prior treatment using RNase A. As shown in Fig. 4A, because 0.05% trypsin detachment removed the proteins on the cell surface, the binding of VEGF G4 to untreated and RNase A-treated cells all increased over 24 h of culture, suggesting an increase in RNA/G4 binding proteins on the cell membrane. The difference in G4 binding to RNase A-treated $versus$ untreated cells also increased markedly over the culture period (Fig. 4B), suggesting a continuous increase in RNA binding on cells throughout the 24-hour culture period. In a subsequent experiment with an extended duration, it was observed that after 24–72 h culture, VEGF G4 binding to both RNase A-treated and untreated cells remained unchanged in 48 h (Fig. S10A). However, by 72 h, VEGF G4 binding to RNase A-treated cells decreased, whereas binding to untreated cells increased, likely due to the reduction of RNA-binding proteins on the cell surface caused by long-term cultivation, and the degradation of RNA adsorbed on the cell surface.

Given that the cells were cultured in media supplemented with 10% FBS, the RNA bound to the cell surface could potentially originate from FBS, be released from lysed dead cells, or have been actively secreted by the cultured cells themselves. To elucidate whether the RNA adsorbed on the cell surface originates from the cells themselves or from external sources such as FBS, we investigated the variation in the amount of RNA bound on the surface of cells cultured in an FBS-free medium over time. In the initial experiment, LoVo cells were detached with 0.05% trypsin to eliminate surface proteins, followed by
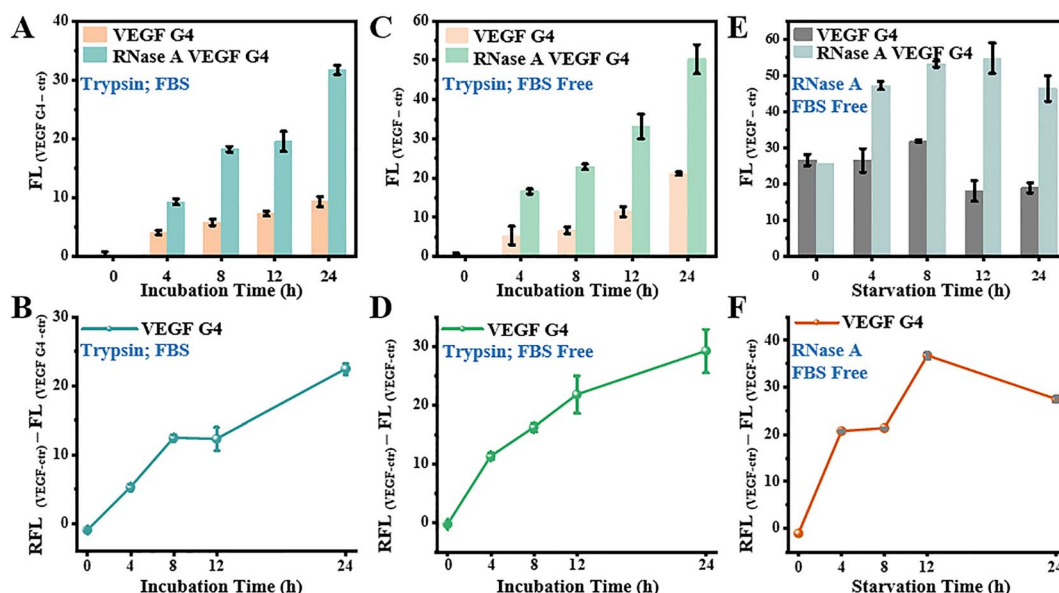

Fig. 4 (A and C) Fluorescence intensity of LoVo cells, digested with trypsin, and cultured in an RPMI1640 medium containing 10% FBS (A) or FBS-free RPMI1640 medium (C) for 0, 4, 8, 12, and 24 h, following treatment with/without RNase A, and then stained by VEGF G4 (200 nM). (E) The fluorescence intensity of LoVo cells treated with RNase A, cultured with an FBS-free medium for 0, 4, 8, 12, and 24 h, following treatment with/without RNase A, and then stained by VEGF G4 (200 nM) (FL, median fluorescence intensity). (B, D and F). The difference in fluorescence intensity between RNase A-treated and untreated cells in Fig. A, C and E (RFL, median fluorescence intensity of RNase A-treated cells; FL, median fluorescence intensity of untreated cells).

cultivation in an RPMI-1640 medium for various durations. Then, the binding of VEGF G4 to LoVo cells was measured under conditions both with and without pretreatment using RNase A. As shown in Fig. 4C, after removal of surface proteins before cultivation, VEGF G4 binding to untreated and RNase A-treated cells all increased over 24 h of culture, suggesting an increase in RNA/G4 binding proteins on the cell membrane. Compared to untreated cells, the binding on RNase A-treated cells showed a markedly higher increase over the same time-frame. The difference in G4 binding to RNase A-treated *versus* untreated cells also increased markedly over culture time (Fig. 4D), suggesting a continuous increase in RNA binding on cells throughout the 24-hour culture period. In a subsequent experiment with a longer duration, it was observed that after 24–72 h in a serum-free medium, VEGF G4 binding to all the treated and untreated cells remained unchanged in 48 h and decreased by 72 h (Fig. S10B). This set of results suggests that RNA-binding proteins (reflected by VEGF G4 binding to RNase A-treated cells) on the cell surface reach equilibrium (saturation) after 24 h and maintain this level until 48 h. However, as cells continue to be cultured in an FBS-free medium, possibly due to nutrient deficiency or changes in cell growth status, the amount of RNA-binding proteins on the cell membrane decreases, leading to a reduction in VEGF G4 binding.

In a subsequent experiment, LoVo cells grown for 24 h (without removing cell surface proteins) were treated with RNase A to remove the RNA bound to the cell surface. After culturing for various durations in an FBS-free medium, VEGF G4 binding was assessed using flow cytometry. As shown in Fig. 4E, VEGF G4 binding on RNase A-treated cells increased steadily untiled 8 h, and remained constant at 12 h, and then slightly decreased at 24 h. In contrast, VEGF G4 binding on untreated cells remained constant until 8 h, and decreased at 12 h, and then remained unchanged. The difference in G4 binding to RNase A-treated *versus* untreated cells also increased markedly until 12 h and slightly decreased at 24 h (Fig. 4F). These results suggest that, without removing RNA-binding proteins from the cell surface and only eliminating surface-bound RNA, the amount of RNA-binding proteins (reflected by G4 binding on RNase A-treated cells) gradually increases over the first 8 h of culture and then reaches saturation. Meanwhile, the levels of RNA binding on the cell surface (reflected by the binding difference) also increase and saturate by 12 h. VEGF G4 binding to untreated cells begins to decline after 12 h, suggesting that binding sites for VEGF G4 are progressively occupied by the increasing amounts of adsorbed RNA on the cell surface. The above two experiments conducted with an FBS-free medium rule out the possibility that the cell surface adsorbed RNA mainly originates from RNA contained in the FBS. It has been reported that RNA can be secreted extracellularly *via* extracellular vesicles and protein pore translocation.[36,37] To a large extent, RNA is likely to be transported out of cells through these pathways. For instance, nucleolin has been considered as a shuttling protein between the nucleus and cytoplasm.[38–40] Given that a suitable method to verify or exclude the origin of cell surface-adsorbed RNA from dead cell lysis remains unavailable, we cannot rule out this source.

A preliminary profile of RNA bound on the cell surface

To ascertain the profile of RNA bound on the cell surface, the nucleic acids were removed from the cell surface proteins with trypsin, and extracted by the phenol/chloroform method. Agarose gel electrophoresis revealed that the extracted nucleic acids were predominantly in the size range from 20–100 nt (Fig. 5A), which was further confirmed by the capillary electrophoresis analysis before transcriptome sequencing (Fig. 5B). This main nucleic acid band can be degraded completely by RNase A but not by DNase I (Fig. 5A). In two other independent experiments, in addition to the main band of 20–100 nt that could be degraded completely by RNase A, a small amount of longer bands ranging from 1000–4000 nt were also detected (Fig. S11) and the longer bands could be completely degraded by DNase I and could not be completely degraded by RNase A (Fig. S12). These results indicate that the RNAs adsorbed on the cell surface are short RNA fragments. The extracted cell surface protein-adsorbed RNA was shown to competitively inhibit the binding of FAM-labeled VEGF G4 to LoVo cells treated with or without RNase A, further confirming their interaction with shared binding sites (Fig. S13). The extracted RNA fragments were then subjected to PE100 paired-end sequencing. However, the sequencing outcomes from three separate experiments lacked consistent reproducibility in RNA sequences, which may be due to random and transient adsorption of RNA with a large library size, as well as inconsistencies in the types and quantities of RNA adsorbed on the surface of cells cultured in different batches. In addition, these adsorbed RNAs were relatively short, with a wide length range (20–100 nt), and coupled with their randomness, they have a significant impact on the sequencing process (such as adapter ligation, reverse transcription, PCR amplification and sequencing). The low reproducibility of the sequencing results may also suggest that the RNA adsorbed on the cell surface lacks sequence specificity and a fixed origin, and they are merely random RNA fragments that randomly bind to the cell surface.

Despite the low reproducibility across the sequencing results, we selected the three most frequently occurring sequences from the first sequencing results, synthesized these RNAs with FAM labels (SSRNA1, SSRNA2 and SSRNA3), and tested their binding to cells. Among them, SSRNA2 was identified in all three sequencing results, while SSRNA1 and SSRNA3 were found in the first and second sequencing results. The SSRNA1, SSRNA2 and SSRNA3 sequences were mapped to the non-coding RNA databases Rfam 15.00 and the non-coding RNAs defined by the Ensembl database sequentially. It was discovered that SSRNA1, SSRNA2 and SSRNA3 sequences were annotated as the transcripts of TPRG1-AS1, PRICKLE2-DT and AKAP1-DT in humans, respectively. All the transcripts mentioned above are long non-coding RNAs, suggesting that SSRNA1, SSRNA2 and SSRNA3 are fragments of long non-coding RNAs. The cell binding assay revealed that all three RNA sequences could bind to LoVo cells untreated with RNase A, with the binding amount in the order of SSRNA2 > SSRNA3 > SSRNA1, exceeding that of the control sequence ss-ctr (the DNA version of SSRNA2). Upon treatment of LoVo cells with RNase A,
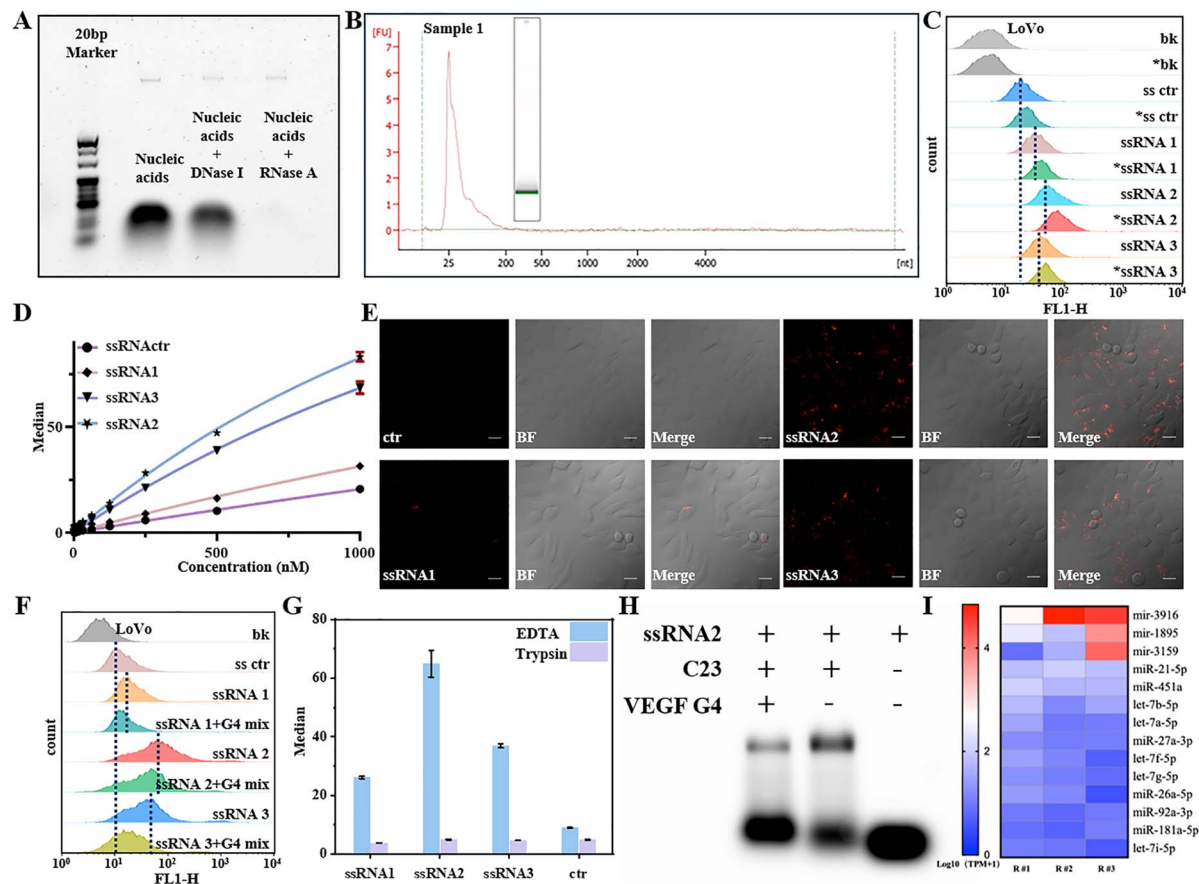
Fig. 5 (A) Agarose gel electrophoresis images of nucleic acids (NA) extracted from the cell surface (sample 1). (B) Capillary electrophoresis analysis of nucleic acids extracted from the cell surface (sample 1). Green color is a marker for 25 nt RNA. (C) Flow cytometry assay of LoVo cells after incubation with FAM-labeled ssRNA 1, ssRNA 2, and ssRNA 3 (800 nM) (* indicates LoVo cells treated with RNase A). (D) Binding curves of FAM-labeled ssRNA 1, ssRNA 2, ssRNA 3 and DNA ctr to LoVo cells. (E) Confocal images of RNase A-treated LoVo cells after incubation with FAM-labeled ssRNA 1, ssRNA 2, ssRNA 3 and ctr sequences (1 μM) (scale bars: 20 μm). (F) Flow cytometry assay of LoVo cells after incubation with FAM-labeled ssRNA 1, ssRNA 2, and ssRNA 3 (800 nM) in the presence or absence of a G4 mix (VEGF G4, AS1411, 3R02-b, c-Kit2 G4, c-Myc G4, 200 nM of each). (G) Binding assay of ssRNA 1, ssRNA 2, and ssRNA 3 (800 nM) to 0.05% trypsin-treated or un-treated LoVo cells respectively. (H) EMSA of the interaction between FAM-labeled ssRNA2 and C23 in the absence and presence of FAM-unlabelled VEGF G4. FAM-labeled ssRNA2 (3 μM) was incubated with nucleolin (C23, 2 μM) and FAM-unlabelled VEGF G4 (6 μM). (I) Repeated miRNA in the transcriptome sequencing results of three parallel groups. Note: in Fig. D, E, F and G, LoVo cells were all treated with RNase A and then with the RNase A inhibitor.

the binding of all three RNA sequences increased, with SSRNA2 showing the most notable enhancement (Fig. 5C). The binding curves (Fig. 5D) and confocal imaging (Fig. 5E) further confirmed the binding of the three RNA sequences to RNase A-treated LoVo cells. The binding of three RNA sequences to RNase A-treated LoVo cells could be competitively inhibited by the G4 DNA mixture (Fig. 5F), further confirming that RNA binds to the same site as DNA G4. When LoVo cells were detached with 0.05% trypsin to remove surface proteins, none of the three RNA sequences were bound (Fig. 5G). Moreover, the EMSA experiment validated the direct interaction between ssRNA2 and nucleolin (C23), while VEGF G4 was shown to compete for their binding (Fig. 5H). From these results, we can infer that the short RNAs bound to cell surface proteins primarily originate from intracellular RNA fragments, and their binding affinity to cell surface proteins is sequence-dependent.

Because the length of most extracted RNA is around 20 nt, which corresponds to the length of microRNAs, we mapped the

extracted RNA to the miRbase database for miRNA annotation and utilized the GraphPad Prism analysis program to examine the miRNAs within the three sequencing results. Our analysis revealed that miRNAs accounted for a very small proportion of the sequences obtained from our sequencing; only 14 human microRNA sequences (including 3 miRNA precursors and 11 mature miRNAs) were identified across all three sequencing results (Fig. 5I). In addition, we also mapped the extracted RNA to the database for other small noncoding RNAs such as siRNA and piRNA. It was found that only a few sequences were matched with piRNAs in the database and none of them matched with siRNA. What's more, the reads of piRNAs in the extracted RNA were much less than miRNAs (data not shown).

Impacts of cell surface RNA on cellular functions

It has been reported that cell surface glycoRNA is inversely associated with tumor malignancy and metastasis.[9] Elimination
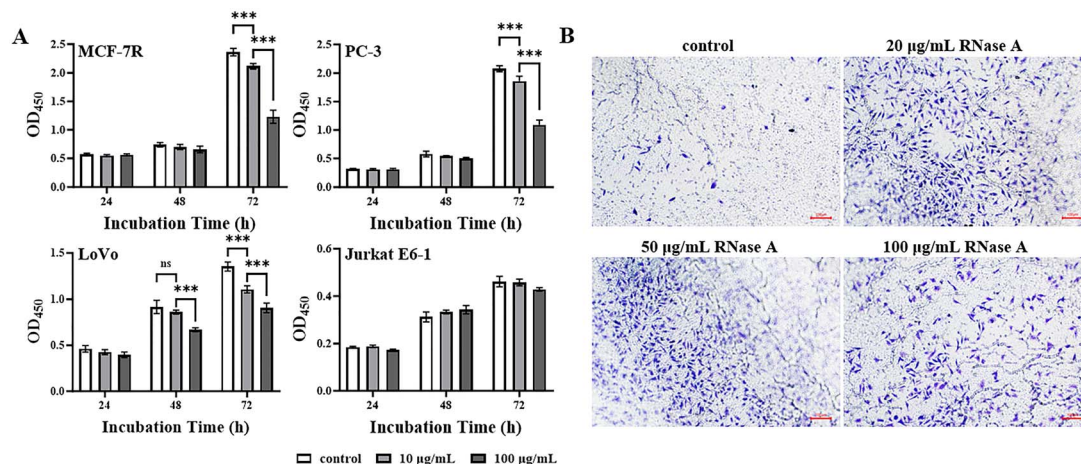
Fig. 6 (A) CCK-8 assay of the proliferative ability of MCF-7R, PC-3, LoVo and Jurkat E6-1 cells treated with 0, 10 and 100 μg mL^{-1} of RNase A (*t*-test, $n = 3$, *$p < 0.05$; ***$p < 0.001$). (B) Transwell migration results of LoVo cells treated with 0, 20, 50 and 100 μg mL^{-1} of RNase A (scale bars: 100 μm).

of cell-surface RNAs by RNase A treatment significantly reduces neutrophil granulocyte recruitment at sites of inflammation *in vivo*.[7] We also conducted a preliminary investigation on the effects of removal of cell surface bound RNA on cell proliferation and migration. The CCK-8 assay showed that culturing MCF-7R, PC-3, and LoVo cells with RNase A for 72 h led to a significant suppression of their proliferation, with the extent of inhibition being concentration-dependent. At the 48-hour mark, only the addition of 100 μg mL^{-1} RNase A exerted a notable inhibitory effect on LoVo cell proliferation, with no significant impact on the other cell lines. Furthermore, RNase A had a negligible impact on the proliferation of Jurkat E6-1 cells (Fig. 6A). The previous experiments have indicated that MCF-7R, PC-3, and LoVo cells exhibit higher levels of RNA adsorption on their surfaces compared to Jurkat E6-1 cells, which have minimal RNA adsorption, suggesting a correlation between RNA bound on the cell surface and cellular proliferation. Furthermore, transwell assays revealed that RNase A treatment significantly enhanced the migratory capacity of LoVo cells (Fig. 6B). These results suggest that cell surface bound RNA might play a role in cell growth and communication with the environment.

Discussion

DNA and RNA are important functional molecules within cells, which can be released into the extracellular fluid through the secretion of living cells and the decomposition of dead cells. It has long been known that the cell surface may adsorb a certain amount of DNA and RNA, including non-specific adsorption through electrostatic interactions, specific adsorption through interactions with specific molecules on the cell surface, and the recently discovered covalent binding of glycosylated RNA on the cell surface.[6,7] However, due to the lack of effective analytical methods, the specific situation of DNA and RNA present on the cell surface is unclear. The aforementioned research preliminarily outlines the situation of RNA binding on the cell surface.

Using dye labeled DNA G4 as molecular probes, we found that the cell surface bound a certain amount of DNA and RNA, with the amount of RNA far exceeding that of DNA. Compared with sequencing-based and hybridization-based methods, the G4 probe-based method is more straightforward and can quickly reflect the total amount of RNA bound to the cell surface. The RNA and DNA G4 bound on the cell surface mainly interact with RNA-binding proteins on the cell surface, for example nucleolin (C23), and thus the change in the amount of DNA G4 bound to the cell surface before and after RNase A treatment can be used to characterize the amount of bound RNA. Preliminary research has found that the amount of surface-bound RNA on different cells also varies significantly, suggesting a large difference in the expression of RNA-binding proteins on the cell surface. After trypsin treatment, the amount of surface proteins on cells gradually increases during subsequent culture, and hence the amount of bound RNA gradually increases within 24 h and then reaches saturation, whereas cells untreated with trypsin, after removing surface-bound RNA with RNase A, show a rapid increase in the amount of surface-bound RNA within 12 h, followed by saturation. The RNA bound to the cell surface is mainly composed of RNA fragments between 20–100 nt in length, including microRNAs. These RNA fragments may originate from RNA transported within the cell or released by dead cells. These adsorbed RNAs on the cell surface may have certain functions, such as participating in the cell's interactions with the extracellular environment.

Of course, the above discussion is merely a preliminary analysis based on the current results. Given the complexity of cell surface components, the dynamic changes of these components during cell growth, and the limitations of current research methods, this study also has certain limitations. (1) Only a few RNA-binding proteins have been detected on the cell surface so far, with nucleolin playing a major role. We believe there are many undetected RNA-binding proteins on different cell surfaces that could have similar effects to the nucleolin. (2) A small number of studies have identified long-chain RNA

bound to the cell surface through sequencing methods. Our findings indicate that the cell surface primarily binds short RNA fragments, thus neglecting the attention to long RNA. (3) The types of cell surface proteins bound by DNA G4 probes and RNA may not be entirely the same; they may only overlap to a certain extent. Therefore, DNA G4 probes may only partially reflect the amount of RNA bound to the cell surface and cannot accurately quantify it. (4) The specific source of RNA adsorbed on the cell surface is still unclear—how is RNA transported out of the cell? Is it fragmented outside or inside the cell? Does it bind to proteins inside the cell and then secreted to the cell surface, or is it first transported out through extracellular vesicles and protein pores and then bound to the cell surface? Or is it mainly released by dead cells? (5) The function of RNA adsorbed on the cell surface is also unclear and requires a large number of experiments for further study.

Author contributions

X. Z. performed the investigation, methodology, and data curation, and wrote the original draft. W. L. performed RNA transcriptome sequencing and data interpretation, and wrote the original draft. W. L. and G. L. performed the Transwell migration experiment. Y. Z., J. S. and Z. L. helped to analyse the data. N. Z., J. Z. and X. L. guided the design of the experiments. D. S. performed supervision and conceptualization, and wrote, reviewed and edited the final manuscript.

Conflicts of interest

There are no conflicts to declare.

Data availability

The raw data can be requested from the corresponding author. Supplementary information: The experimental section, the results and discussion on the optimization of DNA G4 probes, nucleic acid sequences, and supplementary tables and figures. See DOI: https://doi.org/10.1039/d5sc05806f.

Acknowledgements

References

1 E. S. Morozkin, P. P. Laktionov, E. Y. Rykova and V. V. Vlassov, *Ann. N. Y. Acad. Sci.*, 2004, **1022**, 244–249.

2 K. F. Block, E. Puerta-Fernandez, J. G. Wallace and R. R. Breaker, *Mol. Microbiol.*, 2011, **79**, 21–34.

3 T. Janas, T. Janas and M. Yarus, *RNA*, 2012, **18**, 2260–2268.

4 T. Chang, C. Qi, J. Meng, N. Zhang, T. Bing, X. Yang, Z. Cao and D. Shangguan, *PLoS One*, 2013, **8**, e62348.

5 N. Huang, X. Fan, K. Zaleta-Rivera, T. C. Nguyen, J. Zhou, Y. Luo, J. Gao, R. H. Fang, Z. Yan, Z. B. Chen, L. Zhang and S. Zhong, *Genome Biol.*, 2020, **21**, 225.

6 R. A. Flynn, K. Pedram, S. A. Malaker, P. J. Batista, B. A. H. Smith, A. G. Johnson, B. M. George, K. Majzoub, P. W. Villalta, J. E. Carette and C. R. Bertozzi, *Cell*, 2021, **184**, 3109–3124.

7 N. Zhang, W. Tang, L. Torres, X. Wang, Y. Ajaj, L. Zhu, Y. Luan, H. Zhou, Y. Wang, D. Zhang, V. Kurbatov, S. A. Khan, P. Kumar, A. Hidalgo, D. Wu and J. Lu, *Cell*, 2024, **187**, 846–860.

8 H. Liu, X. Li, Y. Ren, Y. Yang, Y. Chen and H. Ju, *J. Am. Chem. Soc.*, 2024, **146**, 8780–8786.

9 Y. Ma, W. Guo, Q. Mou, X. Shao, M. Lyu, V. Garcia, L. Kong, W. Lewis, C. Ward, Z. Yang, X. Pan, S. S. Yi and Y. Lu, *Nat. Biotechnol.*, 2024, **42**, 608–616.

10 E. Wu, X. Guo, X. Teng, R. Zhang, F. Li, Y. Cui, D. Zhang, Q. Liu, J. Luo, J. Wang and R. Chen, *Cell Biochem. Biophys.*, 2021, **79**, 905–917.

11 L. Wang, T. Bing, Y. Liu, N. Zhang, L. Shen, X. Liu, J. Wang and D. Shangguan, *J. Am. Chem. Soc.*, 2018, **140**, 18066–18073.

12 L. Chen, J. Dickerhoff, S. Sakai and D. Yang, *Acc. Chem. Res.*, 2022, **55**, 2628–2646.

13 P. Williams, L. Li, X. Dong and Y. Wang, *J. Am. Chem. Soc.*, 2017, **139**, 12426–12429.

14 H. Shu, R. Zhang, K. Xiao, J. Yang and X. Sun, *Biomolecules*, 2022, **12**, 648.

15 T. Chang, G. Li, Z. Ding, W. Li, P. Zhu, W. Lei and D. Shangguan, *ChemBioChem*, 2022, **23**, e202200405.

16 V. Meier-Stephenson, *Biophys. Rev.*, 2022, **14**, 635–654.

17 Y. Dai, X. Teng, Q. Zhang, H. Hou and J. Li, *Trends Biochem. Sci.*, 2023, **48**, 894–909.

18 T. Bing, L. Shen, J. Wang, L. Wang, X. Liu, N. Zhang, X. Xiao and D. Shangguan, *Adv. Sci.*, 2019, **6**, 1900143.

19 V. González, K. Guo, L. Hurley and D. Sun, *J. Biol. Chem.*, 2009, **284**, 23622–23635.

20 T. Takeiwa, K. Ikeda, K. Horie and S. Inoue, *RNA Biol.*, 2024, **21**, 1–17.

21 B. A. Ozdilek, V. F. Thompson, N. S. Ahmed, C. I. White, R. T. Batey and J. C. Schwartz, *Nucleic Acids Res.*, 2017, **45**, 7984–7996.

22 M. N. Chowdhury and H. Jin, *WIREs RNA*, 2023, **14**, e1748.

23 T. Masuzawa and T. Oyoshi, *ACS Omega*, 2020, **5**, 5202–5208.

24 M. Ghosh and M. Singh, *Nucleic Acids Res.*, 2018, **46**, 10246–10261.

25 N. Vasilyev, A. Polonskaia, J. C. Darnell, R. B. Darnell, D. J. Patel and A. Serganov, *Proc. Natl. Acad. Sci. U.S.A.*, 2015, **112**, E5391–E5400.

26 K. Takahama, K. Kino, S. Arai, R. Kurokawa and T. Oyoshi, *FEBS J.*, 2011, **278**, 988–998.

27 J. Perr, A. Langen, K. Almahayni, G. Nestola, P. Chai, C. G. Lebedenko, R. F. Volk, D. Detrés, R. M. Caldwell, M. Spiekermann, H. Hemberger, N. Bisaria, T. Aiba, F. J. Sánchez-Rivera, K. Tzelepis, E. Calo, L. Möckl, B. W. Zaro and R. A. Flynn, *Cell*, 2025, **188**, 1878–1895.

28 T. Bing, D. Shangguan and Y. Wang, *Mol. Cell. Proteomics*, 2015, **14**, 2692–2700.

29 R. Yagi, T. Miyazaki and T. Oyoshi, *Nucleic Acids Res.*, 2018, **46**, 5894–5901.

30 K. Takahama, C. Sugimoto, S. Arai, R. Kurokawa and T. Oyoshi, *Biochemistry*, 2011, **50**, 5369–5378.

31 X. Liu, W. Mei, V. Padmanaban, H. Alwaseem, H. Molina, M. C. Passarelli, B. Tavora and S. F. Tavazoie, *Mol. Cell*, 2022, **82**, 2604–2617.

32 S. Yang, S. T. Warraich, G. A. Nicholson and I. P. Blair, *Int. J. Biochem. Cell Biol.*, 2010, **42**, 1408–1411.

33 M. Saluri, A. Leppert, G. V. Gese, C. Sahin, D. Lama, M. Kaldmae, G. Chen, A. Elofsson, T. M. Allison, M. Arsenian-Henriksson, J. Johansson, D. P. Lane, B. M. Hallberg and M. Landreh, *PNAS Nexus*, 2023, **2**, 303.

34 A. Ghosh, S. P. Pandey, D. C. Joshi, P. Rana, A. H. Ansari, J. S. Sundar, P. Singh, Y. Khan, M. K. Ekka, D. Chakraborty and S. Maiti, *Nucleic Acids Res.*, 2023, **51**, 9415–9431.

35 M. S. Taha and M. R. Ahmadian, *Cells*, 2024, **13**, 1266.

36 H. Valadi, K. Ekström, A. Bossios, M. Sjöstrand, J. J. Lee and J. O. Lötvall, *Nat. Cell Biol.*, 2007, **9**, 654–659.

37 E. R. Burka, W. Schreml and C. J. Kick, *Biochemistry*, 1967, **6**, 2840–2847.

38 C. Zhuo and X. XinHua, *Saudi Med. J.*, 2016, **37**, 1312.

39 F. Tonello, M. L. Massimino and C. Peggion, *Cell. Mol. Life Sci.*, 2022, **79**, 271.

40 R. A. Borer, C. F. Lehner, H. M. Eppenberger and E. A. Nigg, *Cell*, 1989, **56**, 379–390.